

# Computer Simulation Studies on the Polymer-Induced Modification of Water Properties in Polyacrylamide Hydrogels

Paulo A. Netz\* and Thomas Dorfmueller

Fakultät für Chemie, Physikalische Chemie I, Universität Bielefeld, Postfach 100131,  
33501 Bielefeld, Germany

Received: February 5, 1998

The interactions between polyacrylamide and SPC/E water molecules in polymer gels and solutions were analyzed using computer simulations. Several polymer structures with different concentrations, connectivity characteristics, and pore sizes were used in order to investigate different polymer environments. It was shown that the structure of water was strongly modified in the presence of the polymer. This polymer-induced modification could be characterized in a very detailed way using the spatial distribution function, which considers both the distance as well as the orientation of the water molecules relative to the amide side groups. The dynamics of water, as manifested in the translational and rotational diffusion and residence probability of water is slowed down in the presence of the polymer. The strongest modifications are found in the shell of bound water, but also long-ranged effects were detected. The hydrogen bonds in the vicinity of amide side groups become stronger and longer lived. By setting the partial charges in the amide side groups to zero in some systems, artificial apolar polymer network model systems were defined, whose influence on the structure of water is remarkably different from the influence of the polar networks, although their influence on the transport properties of the surrounding water molecules was found to be quite similar.

## 1. Introduction

Hydrogels belong to the most important materials, both as biological and as technological building blocks. The broad range of applications is related to the properties of hydrogels, between liquid and solid. Recently, it has been postulated to use them as chemomechanical systems or intelligent materials, making use of their peculiar mechanical properties and sensitive response to small variations in temperature and solvent composition.<sup>1–3</sup> Among the synthetic hydrogels the polyacrylamide (PAA) gels, built from acrylamide monomers, and cross-linked by bisacrylamide molecules,<sup>1</sup> certainly belong to the most important ones. They are used in industries, in analytical techniques such as electrophoresis, and in other applications.

The interactions between polymer and solvent molecules, especially the hydrogen bonds<sup>4</sup> and electrostatic interactions, but also geometrical constraints, hydrophobic effects,<sup>5</sup> van der Waals interactions, and the entropical disturbance of the water structure, play a very important role in determining the properties of polyacrylamide gels.

The mutual influence of polymer and solvent is also a key factor in the determination of phase transitions<sup>6</sup> and transport properties of a gel as translational and rotational diffusion coefficients<sup>7</sup> and residence time of water molecules. In the study of the diffusion of weak-interacting particles geometrical considerations such as in the theories of obstruction effect<sup>8–12</sup> can yield a good description for several kinds of gels and solutions, but the diffusion of small molecules and even more the diffusion of the solvent molecules cannot be described satisfactorily. In these systems it is known that the detailed chemical nature of diffusing molecules and their specific

interactions with the polymer play a significant role, and it seems more appropriate to explain the alteration of the transport properties in terms of the modification of the properties of the solvent due to the presence of the polymer,<sup>10,13</sup> the polymer-induced alterations of the solvent properties. Among these properties the local frictional properties of the solvent in the gel may differ strongly from the viscosity of the pure solvent.<sup>10</sup>

The alteration of solvent properties, being a rather local effect, can be better investigated by rotational diffusion than by translational diffusion.<sup>10</sup> Investigations about the dynamics of rotating polyphenyl 2 (PP2) probe molecules show<sup>14</sup> that the reorientation times in pure solvent and solvent mixtures are nearly independent of the quality of the solvent or mixture. In the presence of polyacrylamide gels, however, a strong dependence was detected.<sup>13</sup> This effect seems to be related to a polymer-induced modification of the friction properties of the solvent, characterized by an effective microviscosity, which is enhanced in the presence of polymer. The polymer-induced enhancement of the microviscosity depends strongly on the nature of the solvent.<sup>13,15</sup> Investigations of the polymer-induced modification of the solvent properties by analyzing the reorientation of small molecules as probe<sup>16</sup> have shown, however, that if the size of the probe molecule is comparable with the size of solvent molecules, the effect of the polymer is measurable but much smaller than the effect detected by a larger probe molecule. The mobility of water in hydrogels is, however, significantly lower than in pure water, according to diffusion experiments<sup>7</sup> and computer simulations.<sup>17,18</sup> It is also expected that the polymer modifies the structure and dynamics of the network of hydrogen bonds, which is to a greater extent responsible for the peculiar properties of water.

A microscopically detailed and systematic study of the solvent properties in hydrogels could help to understand the influence of the polymer network on the diffusion and thermodynamic

\* Corresponding author. Departamento de Química, Universidade Lutetana do Brasil, ULBRA, Rua Miguel Tostes 101, Bairro São Luiz, 92420-280 Canoas, Brazil.

properties and give some insights to understand some phenomena of technological and biological relevance. A first step in this study is to investigate the behavior of water molecules in the presence of hydrogels. Computer simulation is very adequate for such studies because it is a method that combines the possibility of detailed microscopic investigation with ease of the variation of concentration and molecular structure. Bulk water has been extensively studied by computer simulation.<sup>19–24</sup> Good reviews about this subject can be found in the literature,<sup>4,25</sup> as well as detailed molecular dynamics studies on the interaction between polymer and water in hydrogels.<sup>17,18,26,27</sup>

The separate analysis of the geometric and electrostatic interactions is in addition a very important step in understanding the microscopic properties of polyacrylamide hydrogels and constitutes an interesting topic to be studied by computer simulations. Computer simulation studies on the comparison between the effect of hydrophobic and hydrophilic surfaces on structural and dynamical properties of water have been carried out by Lee and Rossky.<sup>28</sup> They found that the surface-induced perturbation of structural and dynamical properties of water is mild and short-ranged, somehow more pronounced on hydrophilic surfaces, but the residence times show little sensitivity to the nature of the surface.

In this work we present results of molecular dynamics simulations of polyacrylamide hydrogels. The interaction centers of polymer and water molecules are modeled with atomistic detail. Several polymer structures and concentrations were investigated, in a broad temperature range. Varying the charge parameters of the force field, we were able to investigate separately the influence of geometrical constraints and electrostatic interactions.

We have analyzed the structure of water and hydrogen bonds in polyacrylamide gels and solutions, focusing our attention on the study of the radial and spatial distribution functions and on the environment-dependent properties of water, as well as the dynamics of water: translational and rotational diffusion, residence times, and hydrogen bond correlations.

## 2. Simulation Details

**2.1. Network Formation.** We have investigated the structure and dynamics of water in polyacrylamide hydrogels by using Monte Carlo and molecular dynamics simulations. Model polyacrylamide hydrogels at several concentrations and temperatures have been considered. The initial polymer network structures were generated with our structure generation program described elsewhere.<sup>27,29</sup> The calculations were performed on HP-9000 workstations and on a CRAY Y-MP8.

The polymer networks were built stepwise, site-by-site with fixed bond angles and lengths and atomistic detail, in a cubic simulation box with periodic boundary conditions. The united atom convention for CH and CH<sub>2</sub> groups was used. In our network formation model we distribute a chosen number of knots (each bisacrylamide molecule constitutes a pair of bifunctional knots) in a random way on a diamond lattice. Polyacrylamide chains bridging randomly chosen pairs of knots are generated by constructing the main chain stepwise using a modified self-avoiding random walk with a drift to the target knot, with consideration of periodic boundary conditions and with simultaneous construction of randomly oriented side groups. Polymer networks with a range of concentrations and degrees of cross-linking can be built in this way. These networks have characteristics similar to experimental polymer networks, as inhomogeneities and large pores. The generated structures correspond to rather concentrated gels (see Table 1):

**TABLE 1: Polyacrylamide Structures: Length of the Simulation Box, Number of Water Molecules and of Monomers (Bisacrylamide and Acrylamide), and the Polymer Concentration and Global Density**

structure	box length [Å]	$n_W$	$n_{BIS}$	$n_{ACR}$	PAA concentration [g cm <sup>-3</sup> ]	density [g cm <sup>-3</sup> ]
A	23.52	373	2	11	0.139	0.995
B	24.0	360	3	25	0.269	1.048
C	24.6	328	4	41	0.393	1.051
D	24.0	328	4	41	0.424	1.132
E	32.0	885	8	96	0.406	1.214

this concentration problem is indeed a very common drawback of many simulations. We must interpret our results, therefore, as indicating the behavior in concentrated regions of the gel. The geometrical characterization of the structures will be discussed later.

After the structure generation, a Monte Carlo program which we coded (MCMIN) was run, in order to make a preliminary energy minimization. In this MC program and in the following MD program (see below) the intra- and intermolecular potential parameters were taken from the GROMOS<sup>30</sup> force field. A series of short Monte Carlo simulations, beginning with high temperature and lowering the temperature for subsequent simulations, as a kind of simulated annealing, was carried out. After this process SPC/E<sup>31</sup> water molecules were added to the simulation box, and a further energy minimization was carried out also using the Monte Carlo program.

**2.2. Molecular Dynamics Simulations.** The molecular dynamics simulations of polyacrylamide aqueous solutions and hydrogels were performed using our program GELDYN. The simulations were carried out in the NVE ensemble, with the velocity-Verlet integration algorithm<sup>24</sup> using a time step of 1.0 fs, periodic boundary conditions with a cubic simulation cell, and the minimum image convention. The bonds where hydrogens participate—and in the case of water molecules also the H—O—H angle—were constrained to their equilibrium values using the RATTLE algorithm.<sup>32</sup> Long-ranged electrostatic interactions, considering partial point charges, were calculated using Ewald sums.<sup>33,34</sup> Preliminary simulations have shown that the description of the electrostatic interaction as a simple direct sum produces an artificial enhancement in the structure of water and an energy drift. A detailed list of the force field parameters can be found elsewhere.<sup>27,30</sup>

Due to the large number of degrees of freedom, our simulations were comparatively short: after preliminary minimization runs, a 10 000 steps long equilibration phase was followed by a 20 000 steps long production phase; that is, the total production time per simulation was 20 ps. For one system a simulation with duration of 70 ps was also carried out for comparison, with essentially the same results as the corresponding shorter simulation under the same conditions. The configurations were saved every 0.01 ps as trajectory files.

**2.3. Analysis of Structure and Dynamics.** The characterization of the structures and of the internetwork space is of central importance to understand the influence of the polymer on the properties of the solvent. We have used the concept of the nearest-neighbor volume distribution,<sup>29,35–37</sup>  $V_n(r)$ , and the nearest-neighbor volume fraction,  $\phi_n(r) \equiv V_n(r)/V_T$ , that represents the probability that a randomly chosen point in the simulation box lies in a volume region whose distance to the next obstacle is between  $r$  and  $r + dr$ . The nearest-neighbor volume distribution was computed by the direct Monte Carlo method using 10<sup>7</sup> sample points. The distribution of water molecules in different environments was also studied in detail.

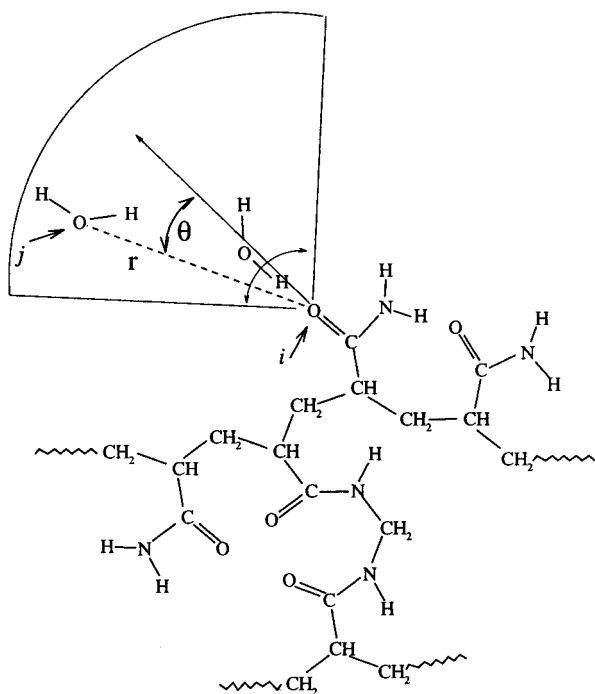


**Figure 1.** Definition of the orientation of water molecules relative to the amide groups in the calculation of the spatial distribution function.

After the simulation, the trajectory file was analyzed in order to calculate the parameters describing structure and dynamics. The structure of water is analyzed in terms of radial distribution functions (site-site pair correlation functions)  $g_{\alpha\beta}$  as obtained by standard methods.<sup>24</sup> The radial distribution function yields an incomplete description of the structure because if the distribution of the molecules is not isotropic, we lose the information concerning the orientation in this orientationally averaged function. The detailed local structure can be studied by means of the spherical harmonic expansion<sup>24</sup> or using an angle-resolved pair distribution function (spatial distribution function<sup>38</sup>). We adopted this last alternative in order to analyze the structure and orientation of water in the vicinity of the polar amide side groups of the polymer gel.

The definition of the spatial distribution function takes into account the orientation  $\Omega$ :

$$g_{\alpha\beta}(r, \Omega) \equiv g_{\alpha\beta}(r, \theta, \phi) \quad (1)$$

In our case, however, we analyze only one angle variable, which is defined according to the orientation of the side group:

$$g_{\alpha\beta}(r, \theta) = \int g_{\alpha\beta}(r, \theta, \phi) d\phi \quad (2)$$

We take as reference angle  $\theta$  the angle between the distance vector—the vector connecting the atom in the side group and the considered atom in the water molecule—and the reference vector, defined by the bond between amide carbon atom and amide oxygen or nitrogen atom. Using this geometrical description, we can take into account the angular information in the form of the spatial distribution function as shown in Figure 1.

The structural properties of water in hydrogels are strongly influenced by the network of hydrogen bonds. A pair of water molecules can be defined to be hydrogen bonded according to energetic<sup>20</sup> or geometric<sup>39</sup> criteria. Both methods yield similar results, but the geometrical criteria are computationally easier and faster to calculate. We defined that a hydrogen bond

between a pair of water molecules occurs when the following conditions are satisfied:

$$R_{OO} \leq 3.60 \text{ \AA}$$

$$R_{HO} \leq 2.45 \text{ \AA}$$

$$\theta \leq 30^\circ$$

where  $R_{\alpha\beta}$  is the distance between the  $\alpha$  atom in the donor and the  $\beta$  atom in the acceptor water molecule and  $\theta$  is the angle  $O_{Ac}O_{Do}H_{Do}$ . Similar definitions were also applied to the hydrogen bonds between polar groups of the polymer and surrounding water molecules. This choice of conditions has proved to be adequate in the investigation of hydrogen bonds in similar systems.<sup>17</sup>

Water molecules were geometrically classified according to their distance to the polymer chain or side groups and according to the polarity of the environment, i.e., whether the water molecules are in the vicinity of hydrophilic amide side groups or hydrophobic chain segments. The borders of the regions defining the hydrophilic or hydrophobic environment are chosen in order to have a small number of molecules on the border, i.e., by taking the first minimum in the radial distribution function. Considering these classifications, the spatial dependence both of the dynamics of water and of the hydrogen bonds was analyzed.

In the calculation of the spatial dependence of dynamical quantities we must take into account the migration of the molecules. The region to which the molecule belongs both at time  $t_0$  and at the time  $t_0 + t$  was considered in the calculation for a given correlation time  $t$ . In the case of hydrogen bond correlations we have, additionally, the possibility of interregional bonds. If one of the atoms belongs to the hydrophilic region, the H-bond is counted to be in the hydrophilic region; the same procedure is applied to the hydrophobic region and the remaining H-bonds (whose atoms belong neither to hydrophilic nor to hydrophobic regions) are classified as bulk H-bonds.

We have calculated the diffusion coefficient of water from the long-time slope of the mean square displacement:

$$D = \frac{1}{6} \lim_{t \rightarrow \infty} \frac{d}{dt} \langle |\mathbf{r}(t) - \mathbf{r}(0)|^2 \rangle \quad (3)$$

The velocity autocorrelation function (VACF) was calculated using standard methods.<sup>24</sup> We have also analyzed this correlation as a function of the distance between the considered water molecule and the polymer chain and taken the integral of the function as an estimate for the spatial dependence of the mobility of water.

The orientational relaxation was investigated by the dipole autocorrelation function, the reorientation of the molecular dipole vector of water:

$$C_R(t) = \frac{\langle \mu(t) \mu(0) \rangle}{\langle \mu(0) \mu(0) \rangle} \quad (4)$$

This autocorrelation was also analyzed as a function of the distance relative to the polymer chain, yielding the spatial dependence of the reorientational mobility of water.

The residence probability  $P_{res}(t)$  was defined as the probability that a water molecule, originally in a definite region, has remained in this region until the time  $t$ . This residence probability was analyzed around amide side groups (hydrophilic environment) and around apolar segments of the chain. It is also possible to define a kind of intermittent residence prob-

ability, similar to the case of hydrogen bond correlations (see below). In this case the molecules are taken into account for the residence correlation at time  $t_0 + t$  even if they have departed from the region in some time interval between  $t_0$  and  $t_0 + t$ . The continuous correlation, where we take into account the first time a water molecule leaves the environment, corresponds to the survival function.<sup>40</sup>

The hydrogen bond autocorrelation function can be defined<sup>41</sup> as a time-dependent autocorrelation function of a state variable  $s_{ij}$  which describes the existence or nonexistence of bonds between a selected donor–acceptor pair  $ij$ .

$$C_{\text{HB}}(t) = \frac{\sum_{ij} s_{ij}(t_0) s_{ij}(t_0 + t)}{\sum_{ij} s_{ij}(t_0)} \quad (5)$$

where  $s_{ij}(t_0) = 1$  if the pair  $ij$  is H-bonded in the time  $t_0$  and 0 otherwise.

Two kinds of correlations can be defined: the intermittent and the continuous correlation. In the former  $s_{ij}(t_0 + t) = 1$  if the bond  $ij$  was found to be present in the time steps  $t_0$  and  $t_0 + t$ , notwithstanding if  $i$  and  $j$  remain H-bonded in the time in between. The long-term rearrangements, i.e., the final breakages, are investigated, ignoring the breakages and reformations at intermediate times. In the definition of the continuous correlation each  $s_{ij}$  is allowed to make just one transition from unity to zero when the bond is first observed to break, not being allowed to return to unity in the case that the same bond reforms.

**2.4. Apolar Systems.** The main effects that influence the diffusion, structure, and dynamics of water in hydrogels originate from long-ranged electrostatic interactions, formation of hydrogen bonds between water and polymer, perturbation of water–water hydrogen bonds, and sterical effects. The latter are mainly due to the formation of polymer cages that restrict the mobility of water molecules. In order to analyze these effects separately, we have proposed a kind of modified gel type, with *apolar chains*, whose side groups have no partial charges or dipoles. The partial charges of water molecules were not changed. With these definitions the geometry of the side groups is the same, and the only difference between these artificial systems and the real polyacrylamide gel networks is that there are no electrostatic interactions between polymer chains and water molecules. Some simulations of pure SPC/E water molecules as well as of PAA structures without solvent were also carried out for comparison.

A list of the parameters that characterize the polyacrylamide structures used in the simulation series is presented in Table 1.

### 3. Results and Discussion

**3.1. Gel Structure.** The generated polyacrylamide structures, listed in Table 1, correspond to concentrated systems or concentrated regions within a larger gel sample. The connectivity characteristics of the structures are very different. Structure A corresponds to nonpercolating polyacrylamide clusters, as in a polymer solution. Structures B, D, and E have increasingly more gel characteristics and constitute polyacrylamide clusters which percolate in one, two, and three dimensions, respectively. Structure C was obtained from structure D by stretching and further relaxation. Structure E has, compared with structure D, a slightly lower polymer concentration, but its spatial distribution of polyacrylamide is more homogeneous.

The relation between the structure of the polymer and the structure of the internetwork space was analyzed using the

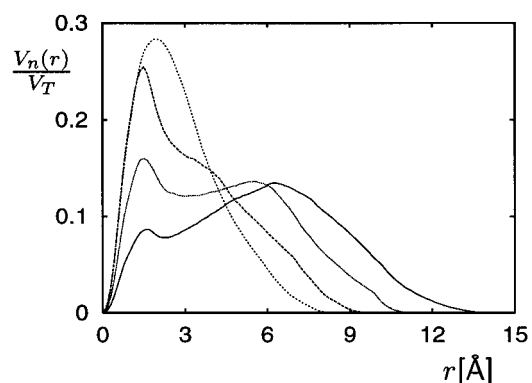


**Figure 2.** Nearest-neighbor volume distribution. Solid line, structure A; dotted line, structure B; heavy dashed line, structure D; and light dashed line, structure E.

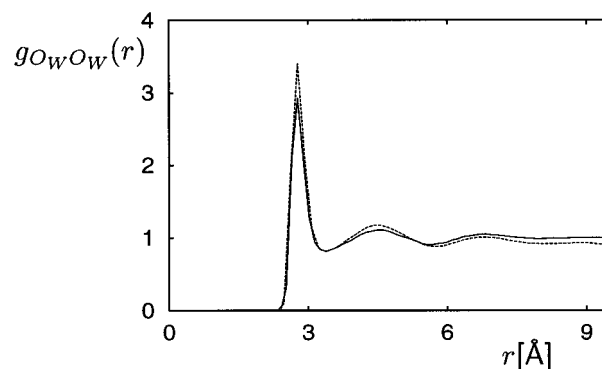


**Figure 3.** Water oxygen–oxygen radial distribution functions  $g_{\text{OwOw}}(r)$  for pure water (solid line) and for the structure D (dashed line), both at 300 K.

nearest-neighbor volume distribution, which estimates the volume of a shell of thickness  $dr$  at a distance  $r$  around a set of reference obstacles. Figure 2 shows the nearest-neighbor volume fraction for the considered structures. We note that when the concentration increases, the structures become more homogeneous, the volume fraction of the larger pores becomes smaller, and only the intramolecular distances, the cages defined by the local structure, and the small pores are important. In concentrated systems an important contribution to the modification of the water properties is due to the disturbance of the connectivity of bulk water, i.e., the impossibility of building a large, percolating cluster of unperturbed water.

Comparison of simulations with and without solvent molecules (not shown) leads to the conclusion that the most important energetic contributions are of electrostatic nature. In the case of a full electrostatic system (*polar chains*) the electrostatic stabilization, i.e., the difference in the energy stemming from electrostatic interactions between hydrogel and polymer without solvent, increases with the polymer concentration (for details see ref 27). A possible immiscibility in the apolar systems was not detected. On the time scale of the simulation only minor structural modifications on the polyacrylamide gels were detected, such as the substitution of intramolecular H-bonds by intermolecular (polymer–water) H-bonds.

**3.2. Pair Distribution Functions.** The influence of the polyacrylamide gel on the structure of water can be analyzed comparing the radial distribution function between oxygen atoms of water  $g_{\text{OwOw}}(r)$  in pure water and in the hydrogel, as shown in Figure 3. This radial distribution function is normalized by the effective density of water,<sup>42</sup> taking into account the dilution due to the polymer. Comparing this radial distribution in hydrogels and in pure water, we see that the maxima and minima

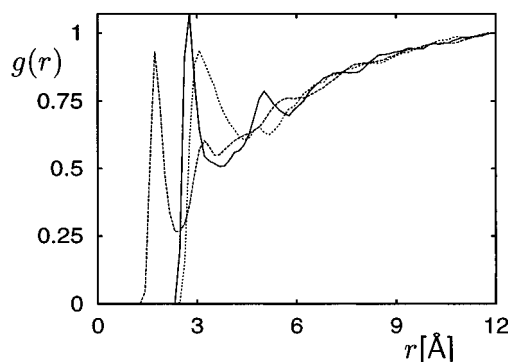


**Figure 4.** Radial distribution functions between atoms of the amide side groups and water molecules for the structure D. Shown are oxygen–oxygen RDF (solid line), oxygen–hydrogen (heavy dashed line), and nitrogen–oxygen (light dashed line).

essentially coincide with that of pure SPC/E water ( $R = 2.8$  Å and  $3.5$  Å, respectively) and that the structure of water as measured by the intensity of the peaks has been slightly enhanced by the presence of the polymer network. It may be argued that the increase of the intensity of the first maximum of  $g_{\text{OwOw}}(r)$  could be due to a decrease of the average number density of water, but in our case we have already taken this decrease in density into account and found that the average density of water (which represents random mixing) decreases faster (from pure water to hydrogel) than the local density. See a similar discussion for aqueous solutions of small molecules in refs 4 and 42. The enhancement effect grows with the polymer concentration and homogeneity.

The effect of the polymer in the structure of water can be better analyzed in the distribution of the water molecules relative to the side groups. Figure 4 shows the radial distribution functions between atoms of the amide side groups and of water:  $g_{\text{OpOw}}(r)$ ,  $g_{\text{OpHw}}(r)$ , and  $g_{\text{NwOw}}(r)$ . The excluded volume effect due to the presence of the chain causes a decrease in the average number density of water molecules close to the amide groups, recognizable by a strong depression in the low-distance region of  $g_{\alpha\beta}(r)$ , even with  $g(r) < 1$ . Nevertheless the definite peaks reflecting the interaction between amide groups and water are clearly visible. The effect is rather short-ranged, but for  $g_{\text{OpOw}}(r)$  a peak at approximately  $5.0$  Å can be seen, related to the second hydration shell. The peaks of the radial distribution functions  $g_{\text{OpOw}}(r)$  become more defined for more concentrated system and broader with increasing temperature.

Polyacrylamide gels are characterized by a strong structure of polymer–water H-bonds, which will be treated in detail later. Both H-bonds between oxygen atoms of the polymer side groups and water hydrogen atoms and those between hydrogen atoms of the polymer side groups and water oxygen atoms are formed. The former are somewhat stronger and shorter ( $r_{\text{O}\cdots\text{H}-\text{O}} < r_{\text{N}-\text{H}\cdots\text{O}}$ ).

**3.3. Spatial Distribution Functions.** The radial distribution function  $g(r)$  represents a detailed microscopic description of the structure in molecular systems and is a kind of orientationally averaged, distance-resolved density. As seen in Figure 4, the anisotropy of the environment and of the distribution of water molecules causes a strong distortion of the radial distribution function between amide atoms and atoms of water. For a detailed molecular characterization we used the angle-resolved pair distribution functions (spatial distribution functions). If we take the side groups as reference for the direction vector (see Figure 1), then water molecules are found preferentially with orientation perpendicular to the chains.

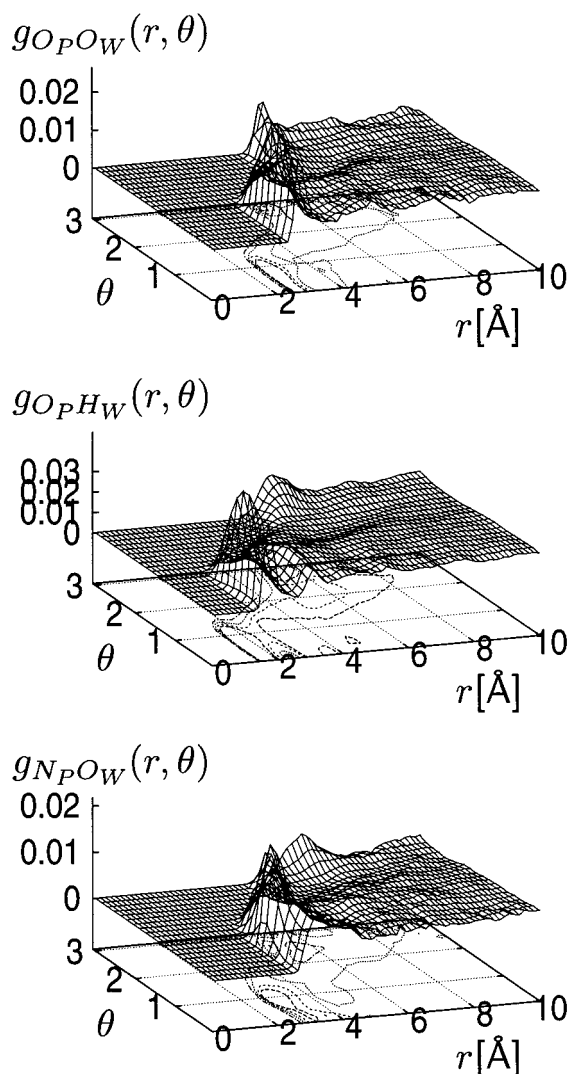


**Figure 5.** Spatial distribution functions  $g_{\alpha\beta}(r, \theta)$  between amide side groups and atoms in the water molecules for the structure D at 300 K:  $g_{\text{OpOw}}(r, \theta)$  (a),  $g_{\text{OpHw}}(r, \theta)$  (b), and  $g_{\text{NwOw}}(r, \theta)$  (c). The angle  $\theta$ , measured in radians, is defined in Figure 1.

Figure 5a–c shows the spatial distribution function  $g_{\alpha\beta}(r, \theta)$  between the atoms in the side groups of the chains and atoms belonging to water molecules. With the help of this representation we can examine the relevant region—perpendicular to the chain, that corresponds to small  $\theta$ -angles—in a very clear way. The effect of the excluded volume of the chain can be seen in all parts of this figure as an extension of the valley up to large distances ( $5.0$ – $6.0$  Å) for angles greater than  $90^\circ$ . The effect of the polymer on the structure of water is short-ranged.

Figure 5a shows the spatial distribution function  $g_{\text{OpOw}}(r, \theta)$  between amide oxygen and water oxygen atoms. Here we can see that the H-bonded oxygen atoms have a very well-defined distance range ( $2.5$ – $3.0$  Å) and also a somewhat fixed orientation, with a maximum at about  $60^\circ$ . This orientation allows the water molecule to form hydrogen bonds with the  $\text{NH}_2$  group of the same amide side group or of neighboring amide groups. A weak structure of the second coordination shell can be recognized in the range of small angles.

Figure 5b shows the correlation between amide oxygen atoms and water hydrogen atoms. Here we can see that there are H-bonds in a broad distribution relative to the angle between the hydrogen bonds and the reference vector ( $\text{C}-\text{O}$ ) up to  $60^\circ$ .

**TABLE 2: Simulation Series. Mean Temperature, Average Fraction of Water Molecules According to Their Distance to the Nearest Polymer Atom and Average Number of Water Molecules in the Vicinity of Hydrophilic Amide Side Groups or Hydrophobic Chain Segments**

simulation	$\langle T \rangle$ [K]	$n_W^{(1)}$	$n_W^{(2)}$	$n_W^{(3)}$	$n_W^{(\text{hphi})}$	$n_W^{(\text{hpho})}$
A/Pol/270	273.6 $\pm$ 5.8	19.1	25.4	32.4	4.02	0.64
A/Pol/280	276.8 $\pm$ 6.5	19.5	26.2	31.6	4.13	0.70
A/Pol/300	292.5 $\pm$ 6.8	19.5	26.4	31.3	4.11	0.68
B/Pol/300	299.4 $\pm$ 5.7	35.6	33.1	31.3	3.27	0.43
C/Pol/280	270.6 $\pm$ 5.7	45.0	31.2	17.8	2.71	0.29
C/Pol/300	297.5 $\pm$ 6.1	44.3	30.9	19.3	2.65	0.32
D/Pol/280	275.9 $\pm$ 5.6	46.7	30.3	19.2	2.93	0.31
D/Pol/300	294.4 $\pm$ 5.8	47.5	30.2	18.7	3.01	0.30
D/Pol/380	378.8 $\pm$ 7.6	49.7	31.6	18.7	3.01	0.27
E/Pol/300	280.7 $\pm$ 3.5	58.0	30.0	11.6	3.52	0.29
A/Apol/280	277.3 $\pm$ 7.0	19.7	23.9	32.6	3.98	0.70
A/Apol/300	300.8 $\pm$ 6.8	18.7	24.3	33.4	3.74	0.74
D/Apol/300	301.7 $\pm$ 5.9	44.2	28.5	22.1	2.75	0.34

The second peak, also over a broad angular distribution, is related to the accompanying hydrogen atom of the donor water molecule.

Comparison of these two figures with Figure 5c, which shows the spatial distribution function between amide nitrogen atoms and water oxygen atoms, indicates the presence of water molecules bound simultaneously to the amide oxygen atoms (water acting as donor) and with the N–H of the same amide group (water acting as acceptor). Here we see that both the angle and the distance range are fixed and very well-defined. The nitrogen atoms act only as donor in the H-bonds, as also confirmed by  $g_{\text{NH}_W}(r, \theta)$  (not shown), which has a strong maximum related to the water hydrogen atom bound with the oxygen atom of the amide side group.

The dependences of the spatial distribution functions on polymer concentration, homogeneity, and temperature confirm the same trends observed in the radial distribution functions and also point out to a short-ranged influence of the polymer chains on the structure of water.

### 3.4. Geometrical Classification of the Water Molecules.

Water molecules were geometrically classified in two ways: according to the minimum distance between the considered molecule and the polymer chains or side groups and according to the polarity of the environment. The latter classification takes into account if the water molecules are in the vicinity of hydrophilic or hydrophobic groups. The water molecule is considered to be in the vicinity of the group if its distance to that group is smaller than the distance of the first minimum of the corresponding radial distribution function. According to this definition, the density of water molecules in the border of the region is kept as small as possible, a very important condition to define residence times.<sup>40</sup> In the hydrophilic amide group both the oxygen and the nitrogen atoms of the amide side groups are considered.

In the classification according to the distance to the chain the minimum distance between a chosen water molecule and the nearest atom belonging to the gel is calculated. This classification is better suited to distinguish between bound and bulk water (and eventually some molecules with intermediate character). It was found that the properties of water depend not only on the polarity of single groups but also on the environment surrounding the groups.<sup>40</sup> In this case a similar approach was applied, considering the mean influence of the chain and of the side groups.

Table 2 summarizes the general static results of the simulation series: temperature and number of waters distributed in regions.

**TABLE 3: Simulation Series. Results of the Analysis of the Hydrogen Bond Structure.  $n_{\text{HB}}^{\text{DA}}$  Means Average Number of Hydrogen Bonds Where D Acts as Donor and A as Acceptor. For  $n_{\text{HB}}^{\text{WW}}$  We Consider Also the Mean Number per Group.  $\langle r_{\text{HB}} \rangle$  Is the Mean Hydrogen–Acceptor Distance and  $\langle \theta_{\text{HB}} \rangle$  Is the Hydrogen Bond Angle Defined in Section 2**

simulation	$n_{\text{HB}}^{\text{P-W}}$	$n_{\text{HB}}^{\text{W-P}}$	$n_{\text{HB}}^{\text{W-W/side group}}$	$\langle r_{\text{HB}} \rangle$ [Å]	$\langle \theta_{\text{HB}} \rangle$ [deg]
A/Pol/270	11	13	9.13	1.87	11.9
A/Pol/280	11	13	9.27	1.88	12.3
A/Pol/300	11	13	9.0	1.89	12.6
B/Pol/300	20	25	6.45	1.88	12.7
C/Pol/280	33	38	5.24	1.89	12.6
C/Pol/300	31	37	4.96	1.89	12.6
D/Pol/280	36	38	5.65	1.87	12.3
D/Pol/300	33	38	5.65	1.88	12.7
D/Pol/380	32	34	5.12	1.91	14.4
E/Pol/300	102	101	6.21	1.86	12.3
A/Apol/280			9.70	1.88	12.3
A/Apol/300			8.80	1.89	12.9
D/Apol/300			5.67	1.88	13.0

It shows the fraction of molecules that lie between 2.0 and 4.0 Å (1), 4.0 and 6.0 Å (2), and 6.0 and 8.0 Å (3) and also the mean number of molecules around a hydrophilic group or a hydrophobic chain segment.

The geometrical distribution of water molecules is almost independent of temperature. The fraction of bound water increases with polymer concentration and with the homogeneity of the polymer. The increase of the homogeneity leads to a higher fraction of solvent-accessible surface area and to a decrease in the fraction of bulk water. For structure E almost 60% of the water molecules are under direct influence of the polymer. The average number of water molecules in the vicinity of hydrophobic and hydrophilic groups (average number per group) decreases with polymer concentration. This effect can be explained by the geometry of the polymer: with increasing concentration the free space around the side groups decreases.

**3.5. Hydrogen Bonds.** The hydrogen bonds were investigated using the geometric criterion discussed in section 2.3. The H-bonds were classified according to their nature (using the convention donor–acceptor): polymer–polymer, polymer–water, water–polymer, and water–water. This last type can be additionally classified according to the environment to which the water molecules belong that share the H-bond.

Table 3 lists the main results regarding the structure of H-bonds. The hydrophilic groups, independent of the polymer concentration, bind strongly almost exactly two water molecules (this can be shown by comparison between number of side groups = number of acrylamide monomers + 2  $\times$  number of bisacrylamide monomers, in Tables 1 and 3) in the polymer–water hydrogen bonds: one acting as acceptor (polymer–water) and the other as donor (water–polymer), with a slight predominance of the latter type. The number of both H-bond types is essentially independent of the temperature. The substitution of water–water hydrogen bonds by polymer–water (and water–polymer) hydrogen bonds seems to be the strongest effect of the polymer on the structure of the H-bonds.

The average number of water–water hydrogen bonds in the vicinity of hydrophilic side groups depends strongly on the concentration and degree of homogeneity of polyacrylamide. This is a rather trivial effect due to the higher accessibility of the side groups at lower polymer concentrations, similar to the above-mentioned decrease of mean number of water molecules around these groups with increasing concentration. The mean distance of the water–water hydrogen bonds (distance between

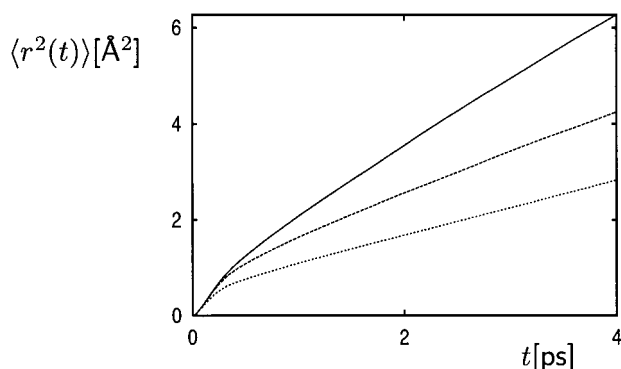


**Figure 6.** Mean square displacement of the center of mass of water molecules in the pure SPC/E water at 300 K (solid line), in the gel structures D at 300 K (heavy dashed line) and E at 280 K (light dashed line).

hydrogen atom and acceptor) is essentially constant, independent both of polymer concentration and of temperature. In the case of mean angle of H-bonds a slight increase with the temperature and no significant dependence on polymer concentration were detected.

**3.6. Diffusion.** Translational diffusion coefficients of water in polyacrylamide hydrogels have been calculated from the mean square displacement. Figure 6 shows the time evolution of the mean square displacement of the center of mass of water, in polyacrylamide gels of different concentrations, compared with pure water. It can be seen that the diffusion is strongly disturbed by the presence of polymer network. The analysis time is not long enough to obtain diffusion coefficients that can be compared to experimental ones, but a somewhat longer simulation with total time of 70 ps and 10 ps of maximum correlation time shows essentially the same results. This longer simulation using structure A at 295 K yields a diffusion coefficient of  $2.07 \times 10^{-5} \text{ cm}^2 \text{ s}^{-1}$ , almost the same as in the shorter simulation.

For systems as complex as water around biological molecules the diffusion is found to be strongly non-Brownian,<sup>43</sup> and the estimated diffusion coefficients may depend on travelled distance or calculation time. Nevertheless a qualitative discussion and analysis of the trends can be made. The corresponding diffusion coefficients show a strong dependence on polymer concentration, as we see in Table 4. The diffusion coefficients decrease with increasing concentration and decreasing temperature. We also carried out simulations of pure SPC/E water at density  $\rho = 0.995 \text{ g cm}^{-3}$  and found diffusion coefficients of  $1.88 \times 10^{-5} \text{ cm}^2 \text{ s}^{-1}$  at 289 K,  $2.33 \times 10^{-5} \text{ cm}^2 \text{ s}^{-1}$  at 299 K, and  $2.82 \times 10^{-5} \text{ cm}^2 \text{ s}^{-1}$  at 304 K. The polymer-induced decrease of the diffusion coefficient attains only a factor of 2.

Compared with the disturbance of the diffusion of large particles,<sup>37</sup> the effect of the polymer network on the diffusion of water is rather limited.<sup>7,16</sup> The effect of the gel is restricted, in the studied systems, mainly to a decrease in the diffusion coefficient: only in very concentrated systems (structure E) was it possible to detect some anomaly in the diffusion, where the mean square displacement shows deviation from the linear dependence on the time. The absence of anomalous diffusion in most systems means that either the influence of polymer on the diffusion of small molecules is not strong enough or the simulated diffusion path is too short. According to this second interpretation, anomalous diffusion can take place, however, on a time scale much longer than covered in these simulations.

Hsu et al.<sup>7</sup> have measured diffusion coefficients of water in polyacrylamide gels at 300 K:  $D = 1.74 \times 10^{-5} \text{ cm}^2 \text{ s}^{-1}$  for polymer concentration of  $0.10 \text{ g cm}^{-3}$  and  $D = 1.06 \times 10^{-5}$

$\text{cm}^2 \text{ s}^{-1}$  for  $0.30 \text{ g cm}^{-3}$ . The agreement between the simulated diffusion coefficients and experimental values is satisfactory. Our values are somewhat larger than the experimental ones, but if we consider that the diffusion coefficient depends on the experimental time scale<sup>44</sup> and shows a trend to diminish for larger observation times, then we can understand the low values of our results as an effect of the short simulation time. The impossibility of a quantitative comparison between simulated and experimental diffusion coefficients does not imply, however, that the trends with concentration or temperature cannot be considered.

**3.7. Velocity Autocorrelation Function.** The center-of-mass velocity autocorrelation function for water molecules in polyacrylamide systems shows only minor effects due to the presence of polymer. The stronger effects can only be detected if we analyze the velocity autocorrelation functions of different water types, classified according to the distance relative to the chains, as explained in section 3.4. Generally speaking we can distinguish between bound and bulk water. In our simulations we have also considered a more detailed description according to the maxima and minima in the pair correlation function. The water molecules are divided in groups whose distance to the polymer chain is between 2.0 and 4.0 Å, 4.0 and 6.0 Å, and 6.0 and 8.0 Å.

The water molecules in the first shell show a more pronounced decrease in the velocity autocorrelation functions, as shown in Figure 7a. In the velocity Verlet algorithm the velocities can be stored as  $\Delta t \times \mathbf{v}$ , and the non-normalized velocity autocorrelation function shown in this figure has the unities of Å<sup>2</sup>. The curve crosses the time axis earlier, and the typical libration shoulder of water is shifted downward. Almost no difference in the dynamical behavior could be detected for water molecules whose distance to the chain were greater than 4.0 Å: the perturbation is strong only in the immediate solvation layer.

The integral of the velocity autocorrelation, in the limit of large times, yields the diffusion coefficient (the integral has the units of Å<sup>2</sup> ps<sup>-1</sup> and due to the normalization must be multiplied by the number of water molecules). Although the velocity autocorrelation functions have not relaxed to zero, we can take the integral of these curves as a qualitative estimate of the distance-dependent diffusion coefficient, as shown in Figure 7b. The errors are, however, much higher than in the estimation of diffusion coefficients using the mean square displacement, and in some cases the fluctuations make it impossible to attribute a definitive value to the coefficient. Table 4 lists the calculated values for the distance-dependent diffusion coefficients. The effect of the polymer on the decrease of water mobility is far more pronounced in the first shell, but it must be regarded as long-ranged: the diffusion coefficients of water in all regions are smaller than for pure water under the same thermodynamic conditions. The bound water reduces the free space available for diffusion and in this way reduces the diffusion coefficient of bulk water. In the structure E, where the regions distant from the chain cannot percolate, this effect is very pronounced. The scattering of the diffusion coefficient values emphasizes the importance of the heterogeneities in determining the transport coefficients.<sup>7</sup>

In the calculation of this distance-resolved velocity autocorrelation function we have also computed the projection of the velocity vector of the considered water molecule on the axis connecting this molecule to the nearest polymer atom, leading to a decomposition in parallel and perpendicular velocity autocorrelation functions, as shown in Figure 8. This decom-

**TABLE 4: Translational and Rotational Diffusion of Water in Polyacrylamide Gels. Diffusion Coefficients and Dipole Reorientational Times Are Analyzed in Their Spatial Dependence, for Water Molecules Classified According to Their Distance to the Polymer in Shells between 2.0 and 4.0 Å (1), 4.0 and 6.0 Å (2), and 6.0 and 8.0 Å (3). Water Molecules Whose Distance to the Chain is More Than 8.0 Å Constitute Only a Very Small Fraction and Were Not Considered in the Averaging**

simulation	$D \times 10^5$ [cm <sup>2</sup> s <sup>-1</sup> ]	$D \times 10^5$ [cm <sup>2</sup> s <sup>-1</sup> ]	$D \times 10^5$ [cm <sup>2</sup> s <sup>-1</sup> ]	$D \times 10^5$ [cm <sup>2</sup> s <sup>-1</sup> ]	$\tau_R$ [ps]	$\tau_R^{(1)}$ [ps]	$\tau_R^{(2)}$ [ps]	$\tau_R^{(3)}$ [ps]
A/Pol/270	0.98	0.6	1.0	1.1	12.17	14.6	11.5	12.1
A/Pol/280	1.36	1.0	1.3-1.4	1.3-1.4	9.82	11.5	9.3	10.3
A/Pol/300	2.13	1.9	2.2	2.3	6.43	8.2	6.5	5.7
B/Pol/300	1.95	1.4	2.0	2.3	6.61	8.1	6.5	5.9
C/Pol/280	1.15	0.8	1.2-1.3	1.2-1.3	12.03	14.2	10.6	10.3
C/Pol/300	1.80	1.6	2.1	2.2	7.35	8.6	6.3	7.0
D/Pol/280	1.11	0.9	1.4	1.7	10.83	14.2	9.2	8.2
D/Pol/300	1.41	1.3	1.7	1.9	7.78	8.9	7.4	6.4
D/Pol/380	5.14	4.3	6.0	6.4	2.19	2.6	1.8	1.6
E/Pol/300	0.95	0.3	0.6	0.9	13.19	16.2	9.9	10.1
A/Apol/280	0.91	0.6	0.9	1.0	14.05	19.1	13.9	13.1
A/Apol/300	2.13	1.8	2.0-2.2	2.0-2.2	5.94	7.4	6.1	5.1
D/Apol/300	1.33	1.1	1.5	1.8	7.54	9.2	6.7	6.5

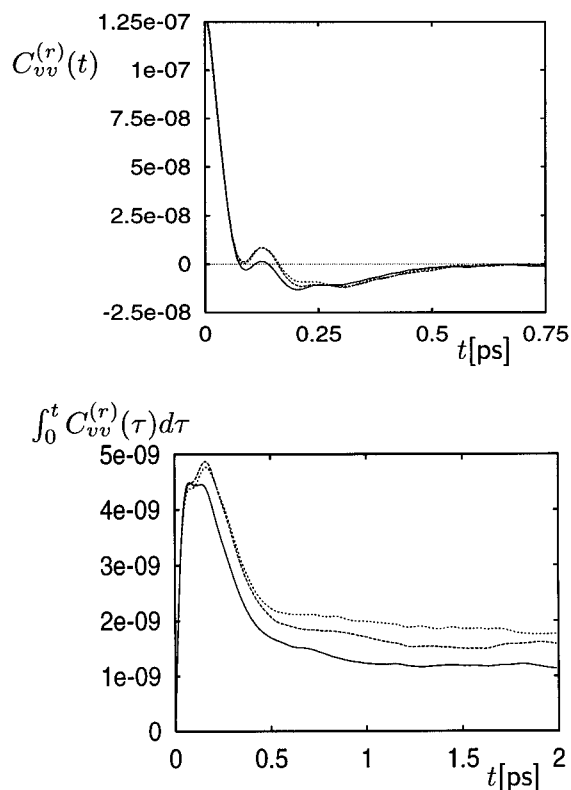


**Figure 7.** Non-normalized velocity autocorrelation functions of water molecules (a) and their integrals (b) for the structure D at 300 K. The water molecules were classified according to their distance to the polymer in shells between 2.0 and 4.0 Å (solid line), 4.0 and 6.0 Å (heavy dashed line), and 6.0 and 8.0 Å (light dashed line).

position loses its validity for large times, because the reference vector changes as the molecule moves, but yields a clear picture of the short-time dynamics: the mobility parallel to this reference vector (perpendicular to the chain) is slowed down stronger than parallel to the chain. The water molecules in the bound water region move preferentially parallel to the surface of the chain. Muegge and Knapp<sup>45</sup> have found a similar behavior in the simulated diffusion of water around BPTI.

**3.8. Orientational Relaxation.** According to experimental investigations,<sup>16</sup> polyacrylamide gels have small effects on the rotational diffusion of tracers whose dimensions are comparable to the dimension of solvent molecules. It is not clear how strongly the rotational diffusion of the water molecules themselves are influenced by the presence of the polymer network.

Figure 9 shows the short-time region of the autocorrelation function for the reorientation of the dipole vector of water in

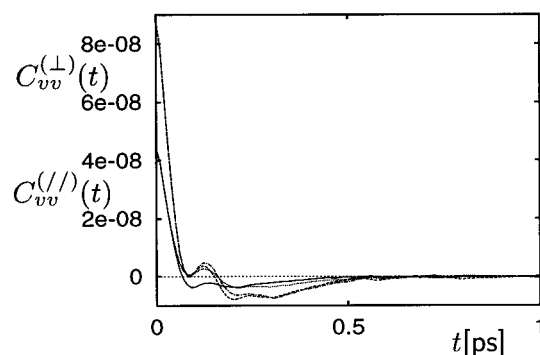


**Figure 8.** Decomposition of the velocity autocorrelation function in components parallel (solid line, between 2.0 and 4.0 Å; dotted line, 4.0 and 6.0 Å) and perpendicular (heavy dashed line, between 2.0 and 4.0 Å, dashed-dotted line, 4.0 and 6.0 Å) to the vector connecting the considered water molecule and the nearest atom belonging to the polymer. The simulation was performed on structure D at 300 K.

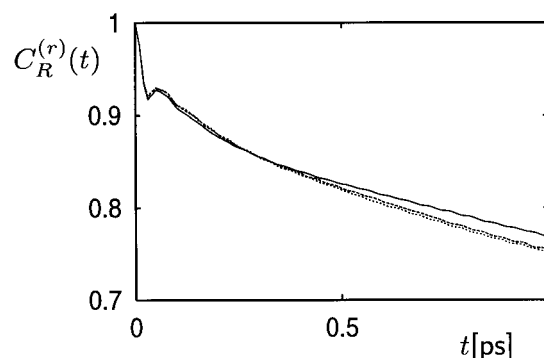


**Figure 9.** Reorientational correlation function for the dipole vector of water molecules classified according to their distance to the polymer (similar to Figure 7) between 2.0 and 4.0 Å (solid line), 4.0 and 6.0 Å (heavy dashed line), and 6.0 and 8.0 Å (light dashed line). The simulation was performed on structure D at 300 K.

polyacrylamide systems, in which the water molecules were classified according to their distance to the chain, in the similar way as in the calculation of the distance-dependent diffusion coefficients. A rapid libration can be seen for times shorter than 0.1 ps, whose typical time and overall appearance seems to be independent of the polymer content and environment. After 0.5 ps the decay of the correlation can be fitted to a single-exponential function, allowing the definition of a reorientational correlation time  $\tau_R$ :

$$C_R(t) = a \exp(-t/\tau_R) \quad (6)$$

Table 4 lists the calculated values of the reorientational correlation time, calculated from a fit between 0.5 and 5 ps.



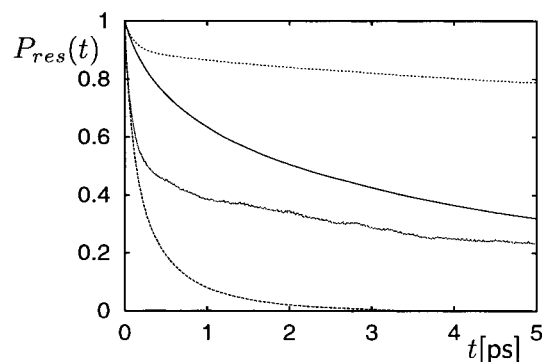


**Figure 10.** Residence probability analyzed according to the continuous correlation definition for water around hydrophilic (solid line) and hydrophobic (heavy dashed line) environments, as well as in the intermittent definition around hydrophilic (light dashed line) and hydrophobic (dotted line) environments, for water molecules in structure D at 300 K.

Surely the higher values (especially when the correlation time is much higher than the analysis time) should be taken rather as qualitative estimates. Our simulations of pure SPC/E water ( $\rho = 0.995 \text{ g cm}^{-3}$ ) yield reorientation times of 5.65 ps at 289 K and 4.64 ps at 304 K. The experimental values of the reorientational time for water are<sup>46</sup> 3.63 ps at 283 K and 2.07 ps at 303 K. The effect of the polymer on the reorientational relaxation is moderately strong, of the same order of magnitude as the effect on the diffusion coefficient, and depends on the gel concentration in the same way.

Analogous to the distance-dependent translational mobilities calculated from the velocity autocorrelation function, we have calculated from  $C_R^{(r)}(t)$  the corresponding reorientational correlation times  $\tau_R$  also as a function of the distance of the molecule to the polymer chain (see Table 4). As in the case of translational diffusion, the molecules in the first shell (bound water) relax much slower than those in the bulk. The effect of the polymer is found, also in the case of reorientation, to be long-ranged.

**3.9. Residence Time Analysis.** Depending on the nature of the environment, water molecules can stay for different lengths of time in a definite region, and this effect can be measured by the residence time correlation  $P_{\text{res}}(t)$ . The residence correlation of water molecules was analyzed around hydrophilic and hydrophobic environments, and the borders of the regions are defined by taking the radius equal to the minimum of the radial distribution function in order that the number density of water on the border should be kept as small as possible. Figure 10 shows the residence correlation around hydrophilic amide groups and hydrophobic chain segments. Both the correlations according to the continuous and also the intermittent definitions are shown.  $P_{\text{res}}(t)$  decreases very slowly around polar groups and fast around the apolar segments. This spreading of residence times (temporal disorder) was found also in water around biological molecules<sup>43</sup> and may lead to anomalous diffusion. The very different decay of the intermittent correlations (compared to the continuous correlations) points to a permanent migration out from and into the region: the molecules that leave the regions diffuse not too far apart and have a high probability of reentering the regions.

For  $P_{\text{res}}(t)$  in the continuous definition it is also possible to calculate a residence time  $\tau_{\text{RT}}$ , by fitting this function to a single exponential for times larger than 0.5 ps. The values are listed in Table 5, but because of the strong deviations from exponential behavior, they should be taken only as qualitative estimates. We see that the residence probability of water is enhanced in

**TABLE 5: Hydrogen Bond Correlation Times According to the Intermittent Definition and Residence Times According to the Continuous Definition for Water Molecules in Polyacrylamide Gels**

simulation	$\tau_{\text{HB}}^{(\text{hphi})}$ [ps]	$\tau_{\text{HB}}^{(\text{hpho})}$ [ps]	$\tau_{\text{HB}}^{(\text{bulk})}$ [ps]	$\tau_{\text{RT}}^{(\text{hphi})}$ [ps]	$\tau_{\text{RT}}^{(\text{hpho})}$ [ps]
A/Pol/270	11.70	12.85	9.74	4.08	1.27
A/Pol/280	8.48	10.10	7.26	3.63	0.85
A/Pol/300	6.58	5.18	4.88	3.59	1.18
B/Pol/300	6.31	5.76	4.82	3.53	0.41
C/Pol/280	10.61	9.98	8.44	5.32	0.53
C/Pol/300	5.98	7.17	5.33	4.84	0.52
D/Pol/280	9.10	11.53	6.18	6.48	0.73
D/Pol/300	6.76	6.31	5.19	5.31	0.65
D/Pol/380	2.06	1.94	1.53	2.91	0.22
E/Pol/300	12.57	11.63	7.97	9.68	1.38
A/Apol/280	13.72	13.01	9.89	1.38	1.05
A/Apol/300	5.88	6.89	4.56	1.28	0.50
D/Apol/300	6.83	6.87	5.50	2.03	0.48

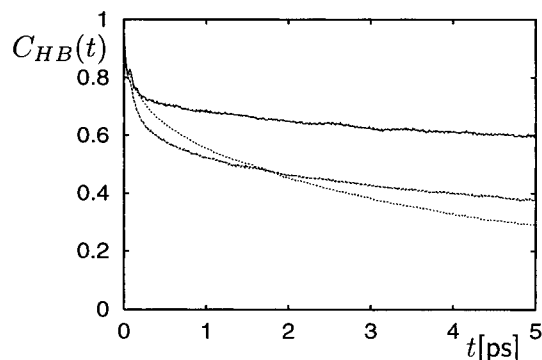
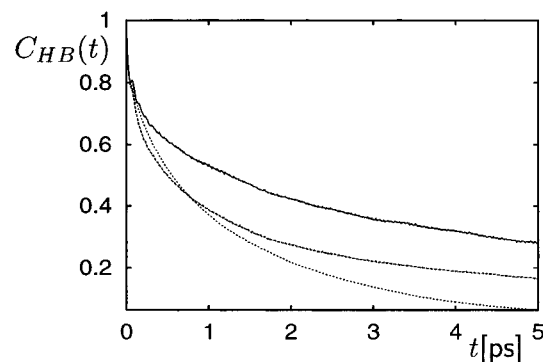


**Figure 11.** Hydrogen bond correlation for polymer–polymer (solid line), polymer–water (heavy dashed line), and water–polymer (light dashed line) for the structure D at 300 K. The H-bonds were calculated according to the continuous (a) and intermittent (b) definitions.

the vicinity of the hydrophilic groups. The residence times depend strongly on temperature and concentration. Bruge et al.<sup>40</sup> found a residence time of 2.4 ps for ST2 water, but if the water molecules are kept fixed, the residence times of water around these grow to approximately 10 ps. The concentration dependence we have found supports the observation that  $\tau_{\text{RT}}$  depends not only on the polarity of single groups but also on the environment surrounding the groups.<sup>40</sup>

**3.10. Hydrogen Bond Dynamics.** The hydrogen bond dynamics was analyzed using the function described in section 2.3. Both intermittent as well as the continuous correlations were calculated for H-bonds between polymer and water and also water–water bonds, the latter classified according to the polarity of the environment (hydrophilic or hydrophobic). Figure 11a,b shows the polymer–polymer and polymer–water H-bond continuous (a) and intermittent (b) correlations. The typical continuous correlations decay much faster than the

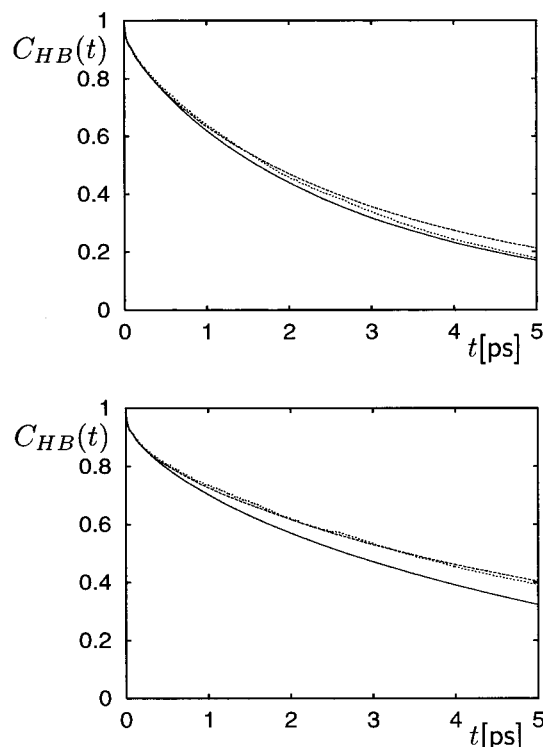


**Figure 12.** Hydrogen bond correlation for H-bonds of water–water in the bulk (solid line), hydrophilic regions (heavy dashed line), and hydrophobic regions (light dashed line) using the continuous (a) and intermittent (b) definitions, in the same conditions of Figure 11.

intermittent ones, approximately an order of magnitude faster.<sup>41</sup> Strong deviations from exponential behavior were found.

The hydrogen bonds in which the polymer participates show a highly nonexponential decay. A typical correlation time is difficult to calculate. The polymer–water and water–polymer correlations cross each other: the decay of the hydrogen bond correlations where the polymer side groups act as donor is stronger for short time scales but becomes slower than the hydrogen bond correlations of water–polymer at about 1.0 ps. This is possibly related to the different nature of the bonds  $N\cdots H-O$  or  $O\cdots H-O$ .

Figure 12a,b shows the H-bond correlations for water in hydrophilic and hydrophobic environments. The decay of these correlations is faster than the decay of the polymer–water hydrogen bond correlations. The intermittent correlations for water molecules in both hydrophilic and hydrophobic environments decay slower than in bulk water: the hydrogen bonds in these environments are longer lived. The fit of the correlations for times longer than 0.5 ps on a single exponential shows strong deviations. Nevertheless correlation times can be calculated and are listed in Table 5. The hydrogen bond decay times in hydrophilic and in hydrophobic regions calculated from the intermittent correlations are comparable, and both are larger than those of bulk water. These intermittent H-bond correlation times are of the same order as the dipole reorientation times.

**3.11. Apolar Systems.** We have also carried out some simulation series in which we do not consider the electrostatic interactions between side groups and water molecules, the apolar chains. Results of these simulations are listed together with the main results in Tables 2–5.

Several of the effects found in the polar systems are also found in the apolar ones. We have seen that also in the apolar case the structure of water as detected by the water–water radial distribution function (not shown) was enhanced. The strongly

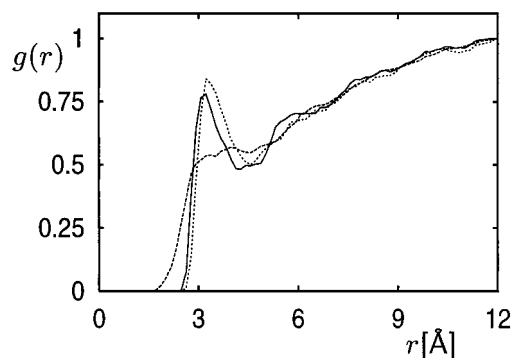


**Figure 13.** Radial distribution functions between atoms of the amide side groups and those of water molecules for an apolar system. The lines represent the same correlations as in Figure 4.

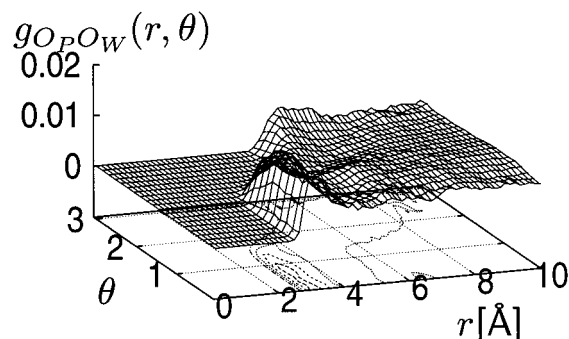


**Figure 14.** Spatial distribution functions between atoms of the amide side groups and of water molecules for an apolar system:  $g_{OpOw}(r, \theta)$ .

different nature of the polymer-induced structural enhancement can be seen in Figure 13, which shows the radial distribution functions  $g_{OpOw}(r)$ ,  $g_{OpHw}(r)$ , and  $g_{NOw}(r)$  for the apolar case. While the first maximum of the distribution function  $g_{OpOw}(r)$  in the polar case (Figure 4) coincides with that of pure water, this peak in the apolar systems is not very well defined and is broad and shifted to larger distances. This suggests a broad, weakly bound hydrophobic water layer in the latter systems.

With the additional information of  $g_{OpHw}(r)$  we see that, in the apolar case, the hydrogen and oxygen atoms of water tend to lie at approximately the same distance relative to the atoms of the side group. The orientation of the water molecules in this case is tangential, as suggested by an enhancement on the structure driven by the hydrophobic effect.<sup>5,42,47</sup>

The spatial distribution functions give us an even clearer picture of the differences in the polymer–water interactions between the apolar and the polar cases. Similar to Figure 5a, Figure 14 shows the spatial distribution functions  $g_{OpOw}(r)$  for the apolar systems. The intensity is much lower than in the case of the polar system, but nevertheless the maxima are clearly recognizable, whose distance and angle ranges are broad. The oxygen–hydrogen spatial distribution function  $g_{OpHw}(r)$  (not shown) is characterized by features in essentially the same distance and angle ranges and confirms that the structure of water molecules in the neighborhood of side groups without charge is predominantly tangential, characteristic of the hydrophobic hydration.

The modifications in the structure of water caused by the apolar systems are very different from those caused by the polar systems. In sharp contrast, we found that the decrease of the diffusion coefficient and the increase of the reorientation time of water molecules in the apolar systems are almost the same as in the polar systems, as can be seen in Tables 4 and 5. Both the hydrophilic electrostatic interactions and polymer–water

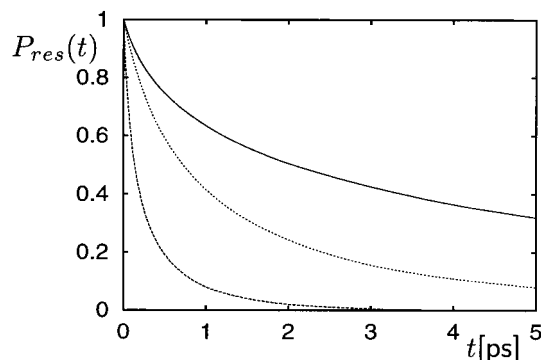


**Figure 15.** Continuous residence probability of water molecules around hydrophilic environments (solid line), apolar side groups of the apolar systems (light dashed line), and apolar chain segments (heavy dashed line).

H-bonds between polar side groups and water molecules as well as the hydrophobic hydration<sup>47</sup> around uncharged groups lead to a reduced mobility<sup>48</sup> of the first shell of water molecules, the bound water. This bound water, on the other hand, slows down the dynamics of the bulk water. The behavior of the velocity autocorrelation functions was found to be almost independent of the polarity of the side groups.

The residence time correlation  $P_{\text{res}}(t)$  around the side groups in the apolar systems decays faster than in the polar case but much slower than in the case of apolar chain segments, as we can see in Figure 15. That means that an adequate geometrical configuration is very important in order that a hydrophobically structured clathrate-like cage of water molecules is built.<sup>5,47</sup>

The hydrogen bond correlations are also found to be almost independent of the polarity of the environment. Hydrogen bonds are stronger and longer lived also in the vicinity of the hydrophobic sites.

#### 4. Conclusions

We have investigated the influence of the polymer on the structure and dynamics of water molecules and hydrogen bonds in polyacrylamide gels and solutions using molecular dynamics simulations.

It was detected that the structure of water is enhanced in the presence of the polymer network, but the effect is short-ranged. The pair distribution functions between atoms of the side group of the polymer and atoms of the water molecules show the strong H-bond-determined structure of water in the presence of the polar side groups.

A spatial distribution function that considers both the distance and the orientation of the water molecules relative to the side groups shows this polymer-induced modification of the solvent structure in a very detailed way without the chain excluded volume effect.

The translational diffusion of water molecules and also the reorientational correlation of their dipole vector slow down in the presence of gel. This effect is strong in the water belonging to the first hydration shell (bound water), and it is found to be not directly dependent on the electrostatics; rather it can be induced both by hydrophilic and by hydrophobic groups. The diffusion perpendicular to the polymer is slowed down more strongly than parallel to the polymer chains.

The study of distance-dependent diffusion coefficients shows that the influence of the polymer on the dynamics of water is long-ranged. This can be understood as an obstruction effect: the presence of bound water reduces the free volume fraction. The slow dynamics of bound water slows down the dynamics

of bulk water. The effect detected is restricted to a decrease in the diffusion coefficient. It is possible that higher concentrations of polymer may lead to anomalous diffusion.<sup>37</sup>

The water residence probability and the hydrogen bond correlation times in hydrophilic and hydrophobic environments are higher than in bulk water. Strong deviations from exponential decay of the correlations were found.

The investigation of artificial apolar gels in the simulation permits us to separate different contributions stemming from sterical factors or hydrophobic and hydrophilic interactions. Side groups without partial charges also induce severe modification in the structure of the solvent, as expected, but the structural modification is very different in this case: A typical tangential geometry of the hydrogen bonds forming a hydrophobic hydration shell was detected. The polymer-induced modification of the dynamics, however, seems to be very similar. Both the molecules that form H-bonds with polar side groups and those that constitute a hydrophobic hydration shell have similar mobilities. The hydrogen bonds become longer lived in the presence of the polymer, independent of the polar characteristics of the environment.

**Acknowledgment.** We gratefully acknowledge the Deutscher Akademischer Austauschdienst, the Fonds der Chemischen Industrie, and the Graduiertenkolleg Strukturbildungsprozesse for financial support, Dr. Michael Buchner and Dr. Wolfgang Eimer for their very valuable suggestions, and Imke Scheppelmann for carrying out some of the SPC/E water simulations.

#### References and Notes

- (1) Tanaka, T. *Sci. Am.* **Jan 1981**, 244, 110.
- (2) De Rossi, D.; Kajiwara, K.; Osada, Y.; Yamauchi, A. *Polymer Gels. Fundamentals and Biomedical Applications*; Plenum Press: New York, 1991.
- (3) Osada, Y.; Ross-Murphy, S. B. *Sci. Am.* **May 1993**, 268, 42.
- (4) Ladanyi, B. M.; Skaf, M. S. *Annu. Rev. Phys. Chem.* **1993**, 44, 335.
- (5) Pratt, L. R. *Annu. Rev. Phys. Chem.* **1985**, 36, 433.
- (6) Tanaka, T. *Phys. Rev. Lett.* **1978**, 40, 820.
- (7) Hsu, T.-P.; Ma, D. S.; Cohen, C. *Polymer* **1983**, 24, 1273.
- (8) Ogston, A. G. *Trans. Faraday Soc.* **1958**, 54, 1754.
- (9) Ogston, A. G.; Preston, B. N.; Wells, J. D.; Snowden, J. McK. *Proc. R. Soc. London A* **1973**, 333, 297.
- (10) Muhr, A. H.; Blanchard, J. M. V. *Polymer* **1982**, 23, 1012.
- (11) Johansson, L.; Skantze, U.; Loeftroth, J.-E. *Macromolecules* **1991**, 24, 6019.
- (12) Johansson, L.; Elvingsson, C.; Loeftroth, J.-E. *Macromolecules* **1991**, 24, 6024.
- (13) Mikosch, W.; Dorfmueller, Th.; Eimer, W. *J. Chem. Phys.* **1994**, 101, 11052.
- (14) Mikosch, W.; Dorfmueller, Th.; Eimer, W. *J. Chem. Phys.* **1994**, 101, 11044.
- (15) Mikosch, W. *Dynamik von Probeteilchen in Hydrogelen. Einfluss der Polymermatrix auf die Transportphänomene*. Ph.D. Thesis, Universitaet Bielefeld, Bielefeld, 1995.
- (16) Biermann, U. M.; Mikosch, W.; Dorfmueller, Th.; Eimer, W. *J. Phys. Chem.* **1996**, 100, 1705.
- (17) Tamai, Y.; Tanaka, H.; Nakanishi, K. *Macromolecules* **1996**, 29, 6750.
- (18) Tamai, Y.; Tanaka, H.; Nakanishi, K. *Macromolecules* **1996**, 29, 6761.
- (19) Barker, J. A.; Watts, R. O. *Chem. Phys. Lett.* **1969**, 3, 144.
- (20) Rahman, A.; Stillinger, F. H. *J. Chem. Phys.* **1971**, 55, 3336.
- (21) Berendsen, H. J. C.; Postma, J. P. M.; van Gunsteren, W. F.; Hermans, J. *Interaction Models for Water in Relation to Protein Hydration*; D. Reidel Publishing Company: Dordrecht, 1981; p 331.
- (22) Berens, P. H.; Mackay, D. H. J.; White, G. M.; Wilson, K. R. *J. Chem. Phys.* **1983**, 79, 2375.
- (23) Jorgensen, W. L.; Chandrasekhar, J.; Madura, J.; Impey, R. W.; Klein, M. L. *J. Chem. Phys.* **1983**, 79, 926.
- (24) Allen, M. P.; Tildesley, D. J. *Computer Simulation of Liquids*; Clarendon Press: Oxford, 1987.
- (25) Ohmine, I.; Tanaka, H. *Chem. Rev.* **1993**, 93, 2545.
- (26) Tamai, Y.; Tanaka, H.; Nakanishi, K. *Mol. Simul.* **1996**, 16, 359.

- (27) Netz, P. A. *Computerexperimente zur Struktur, Dynamik und Diffusion in Polyacrylamidgelen*. Ph.D. Thesis, Universitaet Bielefeld, Bielefeld, 1997.
- (28) Lee, S. H.; Rossky, P. J. *J. Chem. Phys.* **1994**, *100*, 3334.
- (29) Netz, P. A.; Dorfmueller, Th. *J. Chem. Phys.* **1995**, *103*, 9074.
- (30) van Gunsteren, W. F.; Berendsen, H. J. C. *Groningen Molecular Simulations (GROMOS) Library Manual*; GROMOS: Groningen, The Netherlands, 1987.
- (31) Berendsen, H. J. C.; Grigera, J. R.; Straatsma, T. P. *J. Phys. Chem.* **1987**, *91*, 6269.
- (32) Andersen, H. C. *J. Comput. Phys.* **1983**, *52*, 24.
- (33) Leeuw, S. W.; Perram, J. W.; Smith, E. R. *Proc. R. Soc.* **1980**, *A373*, 27.
- (34) Heyes, D. M. *J. Chem. Phys.* **1981**, *74*, 1924.
- (35) Pfeifer, P.; Obert, M. *The Fractal Approach to Heterogeneous Chemistry*, chapter Fractals: Basic Concepts and Terminology; John Wiley: New York, 1989; p 11.
- (36) Torquato, S.; Lee, S. B. *Physica A* **1990**, *167*, 361.
- (37) Netz, P. A.; Dorfmueller, Th. *J. Chem. Phys.* **1997**, *107*, 9221.
- (38) Svishchev, I. M.; Kusalik, P. G. *J. Chem. Phys.* **1993**, *99*, 3049.
- (39) Luzar, A.; Chandler, D. *J. Chem. Phys.* **1993**, *98*, 8160.
- (40) Bruge, F.; Parisi, E.; Fornili, S. L. *Chem. Phys. Lett.* **1996**, *250*, 443.
- (41) Rappaport, D. C. *Mol. Phys.* **1983**, *50*, 1151.
- (42) Soper, A. K.; Luzar, A. *J. Phys. Chem.* **1996**, *100*, 1357.
- (43) Bizzarri, A. R.; Rocchi, C.; Cannistraro, S. *Chem. Phys. Lett.* **1996**, *263*, 559.
- (44) Pavesi, L.; Rigamonti, A. *Phys. Rev. E* **1995**, *51*, 3318.
- (45) Muegge, I.; Knapp, E. W. *J. Phys. Chem.* **1995**, *99*, 1371.
- (46) Jonas, J.; DeFries, T.; Wilbur, D. J. *J. Chem. Phys.* **1976**, *65*, 582.
- (47) Skipper, N. T. *Chem. Phys. Lett.* **1993**, *207*, 424.
- (48) Sciortino, F.; Geiger, A.; Stanley, H. E. *Nature* **Nov 1991**, *354*, 218.